Increased bone density in sclerosteosis is due to the deficiency of a novel secreted protein (SOST)

Wendy Balemans[1], Martin Ebeling[2], Neela Patel[3], Els Van Hul[1], Pam Olson[3], Marianna Dioszegi[3], Charlemagne Lacza[3], Wim Wuyts[1], Jenneke Van Den Ende[1], Patrick Willems[4], Auristela F. Paes-Alves[5], Suvimol Hill[6], Manuel Bueno[7], Feliciano J. Ramos[7], Paolo Tacconi[8], Frederik G. Dikkers[9], Constantine Stratakis[10], Klaus Lindpaintner[11], Brian Vickery[3], Dorothee Foernzler[11] and Wim Van Hul[1,+]

[1]Department of Medical Genetics, University of Antwerp, Universiteitsplein 1, 2610 Antwerp, Belgium, [2]Pharmaceuticals Division, F. Hoffmann-La Roche Ltd, Basel, Switzerland, [3]Musculoskeletal Research, Inflammatory Disease Unit, Roche Bioscience, Palo Alto, CA, USA, [4]Department of Clinical Genetics, Erasmus University, Rotterdam, The Netherlands, [5]Departamento de Ginecología, Obstetrícia e Reprodução Humana, Universidade Federal de Bahia, Salvador, Brazil, [6]Department of Radiology, Clinical Center, National Institutes of Health, Bethesda, MD, USA, [7]Departamento de Pediatria Radiologia Y Medicina Fisica, Universidad de Zaragoza, Zaragoza, Spain, [8]Istituto di Neurologia Universita di Cagliari, Cagliari, Italy, [9]Department of Otorhinolaryngology, University Hospital Groningen, Groningen, The Netherlands, [10]Unit on Genetics of Endocrinology, National Institute of Child Health and Human Development, Bethesda, MD, USA and [11]Roche Genetics, F. Hoffmann-La Roche Ltd, Basel, Switzerland

Sclerosteosis is a progressive sclerosing bone dysplasia with an autosomal recessive mode of inheritance. Radiologically, it is characterized by a generalized hyperostosis and sclerosis leading to a markedly thickened and sclerotic skull, with mandible, ribs, clavicles and all long bones also being affected. Due to narrowing of the foramina of the cranial nerves, facial nerve palsy, hearing loss and atrophy of the optic nerves can occur. Sclerosteosis is clinically and radiologically very similar to van Buchem disease, mainly differentiated by hand malformations and a large stature in sclerosteosis patients. By linkage analysis in one extended van Buchem family and two consanguineous sclerosteosis families we previously mapped both disease genes to the same chromosomal 17q12–q21 region, supporting the hypothesis that both conditions are caused by mutations in the same gene. After reducing the disease critical region to ~1 Mb, we used the positional cloning strategy to identify the *SOST* gene, which is mutated in sclerosteosis patients. This new gene encodes a protein with a signal peptide for secretion and a cysteine-knot motif. Two nonsense mutations and one splice site mutation were identified in sclerosteosis patients, but no mutations were found in a fourth sclerosteosis patient nor in the patients from the van Buchem family. As the three disease-causing mutations lead to loss of function of the SOST protein resulting in the formation of massive amounts of normal bone throughout life, the physiological role of SOST is most likely the suppression of bone formation. Therefore, this gene might become an important tool in the development of therapeutic strategies for osteoporosis.

INTRODUCTION

Sclerosteosis (MIM 269500) belongs to the group of cranio-tubular bone modelling disorders and is inherited as an autosomal recessive trait. This condition, first described by Truswell (1), is characterized by a generalized skeletal overgrowth, mostly pronounced in the skull and mandible (2) (Fig. 1). The clinical features of sclerosteosis include severe facial distortion, tall stature and hand malformations with syndactyly of the digits, radial deviation of the terminal phalanges and dysplastic or absent nails. Raised intracranial pressure may lead to sudden death in sclerosteosis patients. Sclerosteosis is a rare condition and occurs primarily in the Afrikaner population in South Africa, with more than 40 patients having been described (3). One kindred of mixed ancestry from Maryland (4–7), one family of Brazilian origin (8), one family from New York (9) and a few isolated cases from Senegal (10), Spain (11), Switzerland (12) and Japan (13) have also been described.

Figure 1. Lateral view of a patient from the Brazilian sclerosteosis family (8) showing the characteristic high forehead and the protruding large chin.

Van Buchem disease (MIM 239100) is another sclerosing bone dysplasia with an autosomal recessive mode of inheritance that also belongs to the craniotubular hyperostoses. The radio-logical picture of this condition is very similar to sclerosteosis with a significant thickening of the skull, mandible, clavicles, ribs and diaphysis of long bones (14–16). Van Buchem disease is differentiated from sclerosteosis by the presence of a large

stature and hand malformations occuring in the latter (3). The incidence of van Buchem disease is very low: less than 30 cases have been reported worldwide. In 1976, van Buchem *et al.* (15) described a total of 15 patients of Dutch origin. Eight patients from this study and five additional van Buchem patients described by Van Hul *et al.* (17) have been proven to belong to one extended, highly consanguineous family with a common ancestor in the 18th century. Besides these, one family with four affected siblings (18) and a few isolated cases (19–23) have been described.
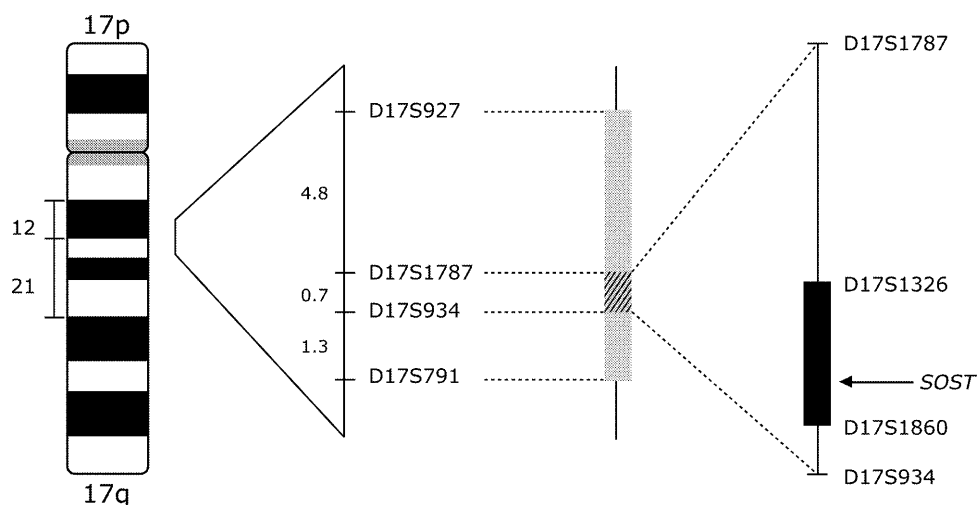
We previously mapped sclerosteosis and van Buchem disease to the same chromosomal 17q12–q21 region (17,24) after performing linkage analysis in the extended Dutch van Buchem family and in an American and Brazilian sclerosteosis family. These results supported the hypothesis postulated by Beighton *et al.* (3) that both conditions are caused by allelic mutations in the same gene with epistatic influences of modifying genes responsible for the phenotypic differences.

In this study, we isolated a novel gene by a positional cloning effort and named this '*SOST*' gene as being the causative gene for sclerosteosis based on the finding of three homozygous loss-of-function mutations in two unrelated sclerosteosis families and one isolated sclerosteosis patient.

RESULTS

Genetic refinement of the candidate disease gene interval

The van Buchem disease gene was previously mapped to an interval of 0.7 cM between D17S1787 and D17S934 (17), whereas the candidate region for the sclerosteosis gene (24) was delineated between D17S927 and D17S791 spanning a 6.8 cM region that completely includes the van Buchem candidate region (Fig. 2). In an attempt to localize the key recombinants more precisely, we performed further linkage analysis on the Dutch van Buchem family using additional genetic markers selected from physical maps of the chromosomal region 17q12–q21 (25–27). This allowed us to refine the candidate

Figure 2. Genetic map of the chromosomal 17q12–q21 region showing the previously described, overlapping sclerosteosis (shaded) and van Buchem (striped) linkage regions. Distances between genetic markers are in centiMorgans (cM). At the right, the reduced candidate gene interval between D17S1326 and D17S1860 is presented in black with the localization of the newly identified *SOST* gene.

region to ~1 Mb of genomic DNA, flanked by markers D17S1326 (proximal) and D17S1860 (distal) (Fig. 2).

Identification of the disease causing gene

In order to identify the disease gene(s), mutation analysis was performed on several known genes and expressed sequence tags (ESTs) from the reduced candidate region without finding any mutations. Simultaneously, ~350 kb of genomic sequence derived from three genomic clones (hCIT.501_O_10, GenBank accession no. AC004149; HRPC905N1, GenBank accession no. AC003098; hCIT.96_E_2, GenBank accession no. AC002094) were screened with exon prediction programs (28). These indicated the presence in these three genomic clones of seven known genes (MOX1, VHR phosphatase, dlg3, vitronectin precursor, EDP1, cytokeratin 18 and PPY) and about 25 high scoring predicted exons. Mutation analysis finally revealed sequence variations in sclerosteosis patients in one putative exon located in the genomic sequence HRPC905N1. A man–mouse cross comparison with the homologous mouse genomic sequence (RP23-346P7, GenBank accession no. AC012296) gave an impressive degree of conservation, confirming the putative coding capacity of this exon. GenScan predicts from the genomic sequence that this exon belongs to a two-exon gene, with *P*-values of 0.999 for both exons.
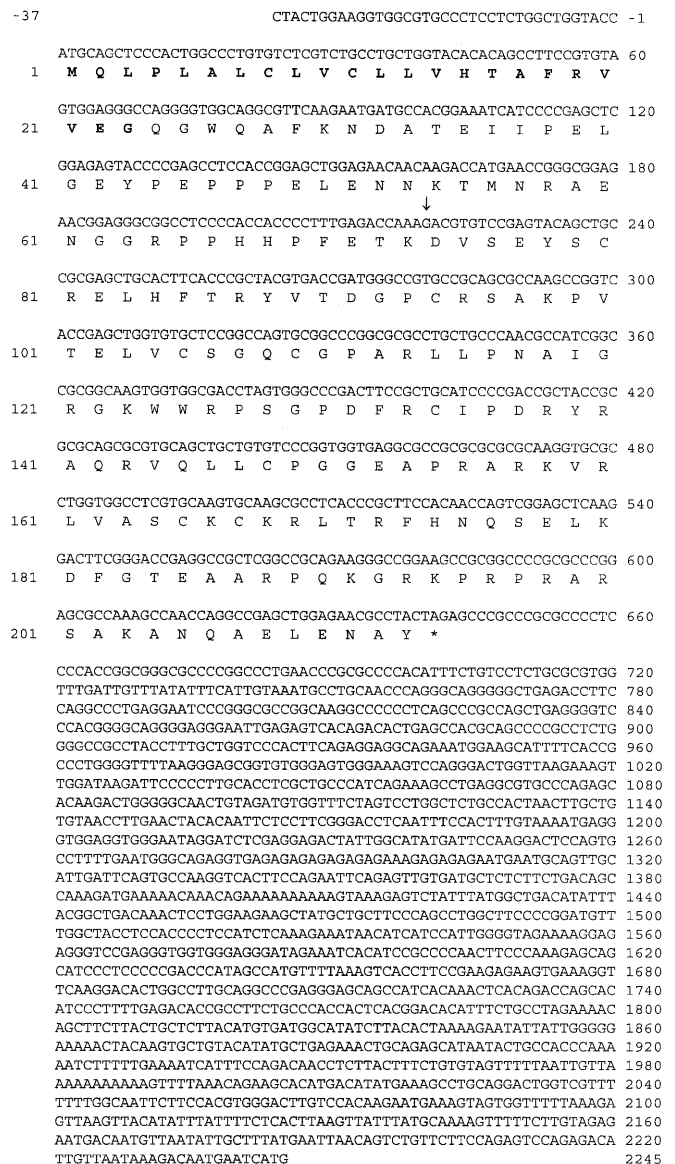
Isolation and characterization of *SOST* cDNA

Confirmation of the GenScan exon prediction results was obtained by the isolation of a putative full-length cDNA clone of ~2.26 kb after screening a human kidney cDNA library (Clontech). Sequence analysis of this cDNA clone revealed an open reading frame of 642 bp and the presence of a clear poly-adenylation signal (AATAAA) at the end of the 3′ untranslated region (UTR) followed by a poly(A) stretch (Fig. 3). 5′- and 3′-RACE experiments resulted in a sequence of 37 bp upstream of the start codon (Fig. 3) but did not reveal any additional sequence at the 3′-side than is included in the isolated cDNA clone. At the genomic level the gene spans ~5 kb for two exons with the consensus GT and AG dinucleotides at the splice sites (Fig. 4).

Mutation analysis of the *SOST* gene

Direct sequencing of the *SOST* gene revealed three different mutations in sclerosteosis patients; none of them was found in control samples. In the two inbred sclerosteosis families used to localize the sclerosteosis gene (24), different homozygous nonsense mutations were found in exon 2 of the *SOST* gene. A Trp124X mutation was identified in all patients from the Brazilian family whereas an Arg126X mutation was found in the American family (Fig. 4). Both mutations cause premature stop codons. An isolated sclerosteosis patient from Senegal (10) has a homozygous splice site mutation (IVS1+3 A→T) (Fig. 4), which causes the consensus value (29) of this splice site to drop from 0.854 for the wild-type sequence to 0.761 for the mutant sequence.

Extensive mutation analysis including the complete gene, the intron sequences, sequences 5′ upstream of the gene and the complete 3′ UTR did not result in the identification of a mutation in a Spanish isolated sclerosteosis patient (11) nor in patients from the Dutch van Buchem family (17).

```
-37                         CTACTGGAAGGTGGCGTGCCCTCCTCTGGCTGGTACC  -1

     ATGCAGCTCCCACTGGCCCTGTGTCTCGTCTGCCTGCTGGTACACACAGCCTTCCGTGTA  60
  1  M   Q   L   P   L   A   L   C   L   V   C   L   L   V   H   T   A   F   R   V

     GTGGAGGGCCAGGGGTGGCAGGCGTTCAAGAATGATGCCACGGAAATCATCCCCGAGCTC  120
 21  V   E   G   Q   G   W   Q   A   F   K   N   D   A   T   E   I   I   P   E   L

     GGAGAGTACCCCGAGCCTCCACCGGAGCTGGAGAACAACAAGACCATGAACCGGGCGGAG  180
 41  G   E   Y   P   E   P   P   P   E   L   E   N   N   K   T   M   N   R   A   E
                                                   ↓
     AACGGAGGGCGGCCTCCCCACCACCCCTTTGAGACCAAAGACGTGTCCGAGTACAGCTGC  240
 61  N   G   G   R   P   P   H   H   P   F   E   T   K   D   V   S   E   Y   S   C

     CGCGAGCTGCACTTCACCCGCTACGTGACCGATGGGCCGTGCCGCAGCGCCAAGCCGGTC  300
 81  R   E   L   H   F   T   R   Y   V   T   D   G   P   C   R   S   A   K   P   V

     ACCGAGCTGGTGTGCTCCGGCCAGTGCGGCCCCGGCGCGCCTGCTGCCCAACGCCATCGGC  360
101  T   E   L   V   C   S   G   Q   C   G   P   A   R   L   L   P   N   A   I   G

     CGCGGCAAGTGGTGGCGACCTAGTGGGCCCGACTTCCGCTGCATCCCCGACCGCTACCGC  420
121  R   G   K   W   W   R   P   S   G   P   D   F   R   C   I   P   D   R   Y   R

     GCGCAGCGCGTGCAGCTGCTGTGTCCCGGTGGTGAGGCGCCGCGCGCGCGCAAGGTGCGC  480
141  A   Q   R   V   Q   L   L   C   P   G   G   E   A   P   R   A   R   K   V   R

     CTGGTGGCCTCGTGCAAGTGCAAGCGCCTCACCCGCTTCCACAACCAGTCGGAGCTCAAG  540
161  L   V   A   S   C   K   C   K   R   L   T   R   F   H   N   Q   S   E   L   K

     GACTTCGGGACCGAGGCCGCTCGGCCGCAGAAGGGCCGGAAGCCGCGGCCCCGCGCCCGG  600
181  D   F   G   T   E   A   A   R   P   Q   K   G   R   K   P   R   P   R   A   R

     AGCGCCAAAGCCAACCAGGCCGAGCTGGAGAACGCCTACTAGAGCCCGCCCGCGCCCCTC  660
201  S   A   K   A   N   Q   A   E   L   E   N   A   Y   *

     CCCACCGGCGGGCGCCCCGGCCCTGAACCCGCGCCCCACATTTCTGTCCTCTGCGCGTGG  720
     TTTGATTGTTTATATTTCATTGTAAATGCCTGCAACCCAGGGCAGGGGGCTGAGACCTTC  780
     CAGGCCCTGAGGAATCCCGGGCGCCGGCAAGGCCCCCCTCAGCCCGCCAGCTGAGGGGTC  840
     CCACGGGGCAGGGGAGGGAATTGAGAGTCACAGACACTGAGCCACGCAGCCCCGCCTCTG  900
     GGGCCGCCTACCTTTGCTGGTCCCACTTCAGAGGAGGCAGAAATGGAAGCATTTTCACCG  960
     CCCTGGGGTTTTAAGGGAGCGGTGTGGGAGTGGGAAAGTCCAGGGACTGGTTAAGAAAGT  1020
     TGGATAAGATTCCCCCTTGCACCTCGCTGCCCATCAGAAAGCCTGAGGCGTGCCCAGAGC  1080
     ACAAGACTGGGGGCAACTGTAGATGTGGTTTCTAGTCCTGGCTCTGCCACTAACTTGCTG  1140
     TGTAACCTTGAACTACACAATTCTCCTTCGGGACCTCAATTTCCACTTTGTAAAATGAGG  1200
     GTGGAGGTGGGAATAGGATCTCGAGGAGACTATTGGCATATGATTCCAAGGACTCCAGTG  1260
     CCTTTTGAATGGGCAGAGGTGAGAGAGAGAGAGAGAAAGAGAGAGAAGATGAATGCAGTTGC  1320
     ATTGATTCAGTGCCAAGGTCACTTCCAGAATTCAGAGTTGTGATGCTCTCTTCTGACAGC  1380
     CAAAGATGAAAAACAAACAGAAAAAAAAAAAGTAAAGAGTCTATTTATGGCTGACATATTT  1440
     ACGGCTGACAAACTCCTGGAAGAAGCTATGCTGCTTCCCAGCCTGGCTTCCCCGGATGTT  1500
     TGGCTACCTCCACCCCTTCCATCTCAAAGAAATAACATCATCCATTGGGGTAGAAAAGGAG  1560
     AGGGTCCGAGGGTGGTGGGAGGGATAGAAATCACATCCGCCCCAACTTCCCAAAGAGCAG  1620
     CATCCCTCCCCCGACCCATAGCCATGTTTTAAAGTCACCTTCCGAAGAGAAGTGAAAGGT  1680
     TCAAGGACACTGGCCTTGCAGGCCCGAGGGAGCAGCCATCACAAACTCACAGACCAGCAC  1740
     ATCCCTTTTGAGACACCGCCTTCTGCCCACCACTCACGGACACATTTCTGCCTAGAAAAC  1800
     AGCTTCTTACTGCTCTTACATGTGATGGCATATCTTACACTAAAAGAATATTATTGGGGG  1860
     AAAAACTACAAGTGCTGTACATATGCTGAGAAACTGCAGAGCATAATACTGCCACCCAAA  1920
     AATCTTTTTGAAAATCATTTCCAGACAACCTCTTACTTTCTGTGTAGTTTTTAATTGTTA  1980
     AAAAAAAAAGTTTTAAACAGAAGCACATGACATATGAAAGCCTGCAGGACTGGTCGTTT  2040
     TTTTGGCAATTCTTCCACGTGGGACTTGTCCACAAGAATGAAAGTAGTGGTTTTTAAAGA  2100
     GTTAAGTACATATTTATTTTCTCACTTAAGTTATTTATGCAAAAGTTTTTCTTGTAGAG  2160
     AATGACAATGTTAATATTGCTTTATGAATTAACAGTCTGTTCTTCCAGAGTCCAGAGACA  2220
     TTGTTAATAAAGACAATGAATCATG  2245
```

Figure 3. Nucleotide sequence and the deduced amino acid sequence of the human *SOST* cDNA. Amino acid numbering is given on the left starting with the initiation methionine. Nucleotide positions are given on the right also beginning at the initiation methionine codon. The signal peptide is given in bold and the intron position is marked with an arrow. The polyadenylation signal (AATAAA) is underlined.

Expression analysis of the *SOST* mRNA

To evaluate the expression pattern of *SOST,* quantitative (qt) TaqMan PCR was performed on a panel of RNAs from 13 different adult human tissues. As illustrated in Figure 5, *SOST* expression is highly restricted and expression levels are quite low, being below the detection limit of northern blots. The highest expression was detected in kidney (2.5% ± 0.2 of GAPDH expression) followed by bone marrow (0.6% ± 0.1 of GAPDH expression). Also some expression in lung, heart and pancreas can be detected. Interestingly, qtPCR analysis revealed *SOST* expression in primary human osteoblasts differentiated for 21 days (0.3% ± 0.02 of GAPDH expression).
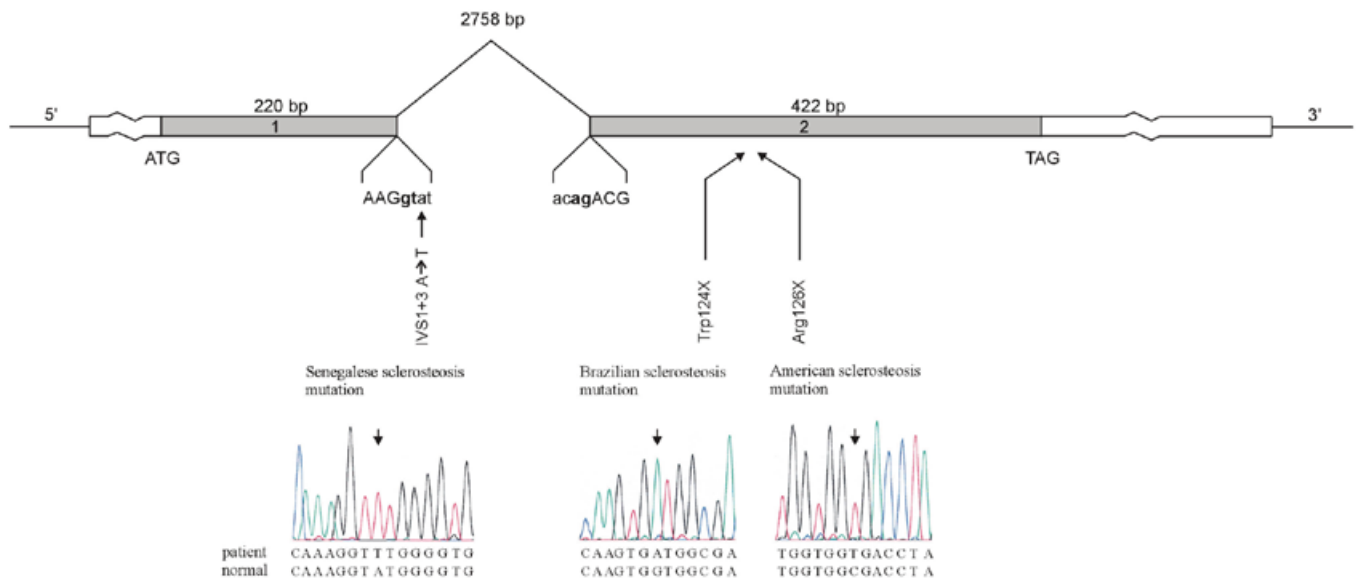
Figure 4. Genomic structure of the *SOST* gene showing the presence of two exons and one intron. Below are the positions, the nature and the electropherograms given for the homozygous mutation found in the sclerosteosis patients.
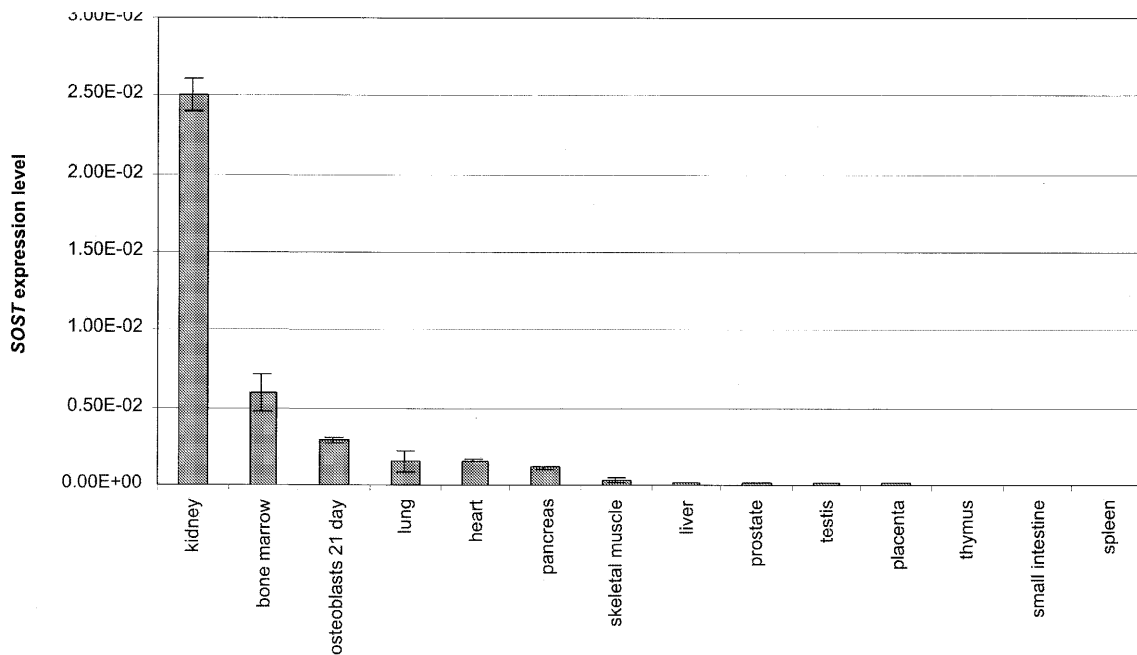
Figure 5. Expression of *SOST* using quantitative TaqMan assay in 13 different human tissues and osteoblasts differentiated for 21 days. All values are normalized to GAPDH expression. Data are expressed as the average of duplicates ± range.
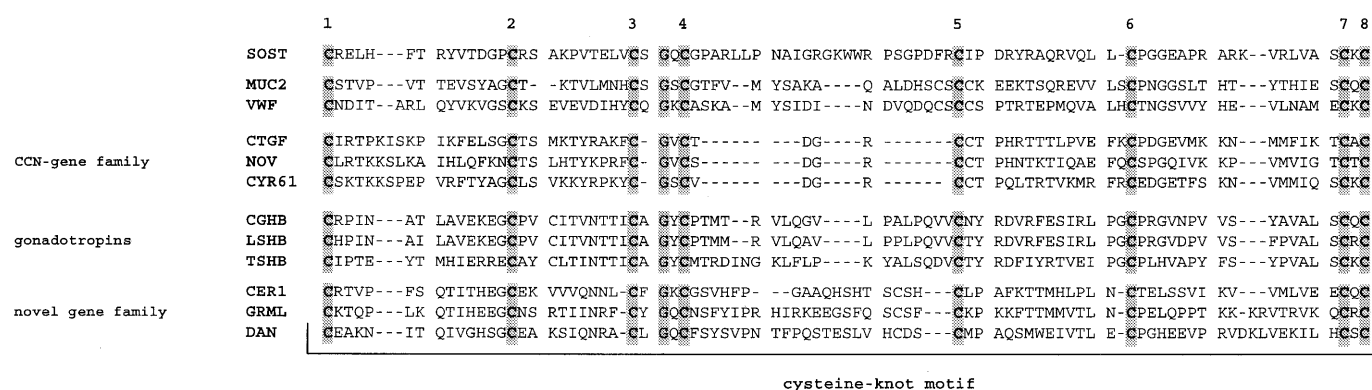
Identification of homologous sequences

Homology searches using the BLAST programs (30) enabled us to identify the mouse ortholog for the *SOST* gene showing an amino acid identity of 87%. This ortholog lies within the sequence of genomic clone RP23–346P7 (GenBank accession no. AC012296), localized on mouse chromosome 11, within the syntenic region of chromosome 17q12–q21. At the same time, one human homologous sequence was found within a genomic chromosome 7 clone (RP11–372J17; GenBank accession no. AC079155), indicating the presence of a gene with an amino acid identity of 36% compared with the *SOST* gene.

Protein structure predictions of SOST

The *SOST* gene encodes a 213 amino acid propeptide with a calculated molecular weight of 24 kDa including a signal

```
                        1                  2            3     4                              5                6                   7  8
        SOST    CRELH---FT RYVTDGPCRS AKPVTELVCS GQCGPARLLP NAIGRGKWWR PSGPDFRCIP DRYRAQRVQL L-CPGGEAPR ARK--VRLVA SCKC

        MUC2    CSTVP---VT TEVSYAGCT- -KTVLMNHCS GSCGTFV--M YSAKA----Q ALDHSCSCCK EEKTSQREVV LSCPNGGSLT HT---YTHIE SCQC
        VWF     CNDIT--ARL QYVKVGSCKS EVEVDIHYCQ GKCASKA--M YSIDI----N DVQDQCSCCS PTRTEPMQVA LHCTNGSVVY HE---VLNAM ECKC

        CTGF    CIRTPKISKP IKFELSGCTS MKTYRAKFC- GVCT------ ---DG----R -------CCT PHRTTTLPVE FKCPDGEVMK KN---MMFIK TCAC
CCN-gene family NOV CLRTKKSLKA IHLQFKNCTS LHTYKPRFC- GVCS------ ---DG----R -------CCT PHNTKTIQAE FQCSPGQIVK KP---VMVIG TCTC
        CYR61   CSKTKKSPEP VRFTYAGCLS VKKYRPKYC- GSCV------ ---DG----R ------CCT PQLTRTVKMR FRCEDGETFS KN---VMMIQ SCKC

        CGHB    CRPIN---AT LAVEKEGCPV CITVNTTICA GYCPTMT--R VLQGV----L PALPQVVCNY RDVRFESIRL PGCPRGVNPV VS---YAVAL SCQC
gonadotropins LSHB CHPIN---AI LAVEKEGCPV CITVNTTICA GYCPTMM--R VLQAV----L PPLPQVVCTY RDVRFESIRL PGCPRGVDPV VS---FPVAL SCRC
        TSHB    CIPTE---YT MHIERRECAY CLTINTTICA GYCMTRDING KLFLP----K YALSQDVCTY RDFIYRTVEI PGCPLHVAPY FS---YPVAL SCKC

        CER1    CRTVP---FS QTITHEGCEK VVVQNNL-CF GKCGSVHFP- --GAAQHST SCSH---CLP AFKTTMHLPL N-CTELSSVI KV---VMLVE ECQC
novel gene family GRML CKTQP---LK QTIHEEGCNS RTIINRF-CY GQCNSFYIPR HIRKEEGSFQ SCSF---CKP KKFTTMMVTL N-CPELQPPT KK-KRVTRVK QCRC
        DAN     CEAKN---IT QIVGHSGCEA KSIQNRA-CL GQCFSYSVPN TFPQSTESLV HCDS---CMP AQSMWEIVTL E-CPGHEEVP RVDKLVEKIL HCSC
                                                                                                                     
                                                        cysteine-knot motif
```

Figure 6. Multiple alignment of the cysteine-knot domain of SOST with those from other proteins. The eight cysteine residues (numbered 1–8) and one glycine residue obligate for cysteine-knot formation are shaded. The GenBank accession numbers for the sequences as listed are: AF331844; NP_002448; P04275; NP_001892; NP_002505; CAA72167; P01233; O46483; P01222; NP_005445; AAF06677; P41271.

sequence for secretion (31) in the first 23 residues (Fig. 3). Further screening of the amino acid sequence for functional domains or motifs using the Pfam protein families database (32) revealed the presence of a cysteine-knot motif based on the conservation of nine amino acids (eight cysteines and one glycine) that are essential to form the central cysteine-knot (Fig. 6).

DISCUSSION

A positional cloning strategy was used to identify the defective gene in sclerosteosis and van Buchem disease under the assumption that both conditions are allelic. We refined the previously defined genetic interval to a region of ~1 Mb by further study of the key recombinational events in the extended Dutch van Buchem family. Known genes and ESTs and predicted exons from the candidate region were screened for mutations. We found three loss-of-function mutations in a previously unidentified gene, two nonsense mutations causing a premature stop codon and one splice site mutation. This clearly identifies this gene as the *SOST* gene and as being causative for sclerosteosis. We were not able to identify any disease causing mutations in a fourth isolated sclerosteosis patient from Spain. This can be explained in different ways. First, genetic heterogeneity for sclerosteosis cannot be ruled out at this point. Second, the expression of the *SOST* gene could be influenced by mutations in *cis*-acting regulatory regions or by rearrangements causing a positional effect on the expression of the gene (33). We also believe that the second possibility most probably explains the fact that no mutations were found in the Dutch van Buchem family, despite the fact that the *SOST* gene resides within the small candidate region delineated by linkage analysis in this family. As already illustrated for the *SOX9* and *SHH* genes (33) mutations outside these genes can result in milder phenotypes than mutations in the coding sequence. Alternatively, another (related) gene causing a similar phenotype can be localized in the same chromosomal region. However, we consider this possibility very unlikely also because a major part of the 1 Mb candidate region has already been sequenced without revealing any strong candidate genes.

Since the *SOST* gene is not expressed in leukocytes and due to the unavailability of appropriate tissue material, we were not able to determine the true effect of the splice site mutation in the Senegalese sclerosteosis patient (IVS1+3 A→T). Theoretically, the efficiency of splicing can be calculated in terms of the Shapiro and Senapathy 'consensus values' for the wild-type and the mutant allele (29). It has been illustrated in *LCAMB* (34) and *OTC* (35) that reduction of the consensus values in mutant alleles versus the wild-type causes complete exon skipping since in 96% of all cases a purine is found at the +3 position of 5′ splice donor sites. This raises the possibility for the splice site mutation in the Senegalese patient to cause a similar effect, as the degree of reduction of the consensus value in the *SOST* gene is equal to those found in the *LCAMB* and *OTC* genes.

In the first 23 amino acid residues the SOST protein carries a signal peptide for secretion and the conservation of eight cysteine and one glycine residue in SOST indicates the presence of a cysteine-knot motif, known to participate in dimerization and receptor binding. This motif was first described in the TGF-β gene family (36) and in the connective tissue growth factor (CTGF) (37). Later it has been found in other proteins such as the von Willebrand factor, the mucins, members of the CCN gene family (38), the gonadotropin family (39) and more recently in a novel gene family including gremlin, DAN and cerberus (40). Despite the lack of significant overall sequence similarity, SOST can be aligned to these proteins (Fig. 6) based on the complete conservation of eight cysteine and one glycine residue, which are crucial for the three-dimensional structures of the aligned domains. The different members of this cysteine-knot growth factor super-family form hetero- and/or homodimers before binding to their receptors, and have very divergent biological functions.

In conclusion, evidence is provided that the deficiency of SOST, a novel secreted protein expressed in osteoblasts, leads to the increased bone density in sclerosteosis. The two nonsense mutations and the splice site mutation are loss-of-function mutations. Though the precise function and working of SOST remains unknown, an inhibitory effect on bone formation can be proposed since pathophysiological analysis indicated that sclerosteosis is primarily a disorder of increased

formation of normal bone (7). This definitely makes this protein and its pathway interesting targets for the development of anabolic agents against osteoporosis.

MATERIALS AND METHODS

Patients and families

Patients from the two sclerosteosis families from the US (4–7) and Brazil (8), the Dutch van Buchem family (17,15) and the two isolated sclerosteosis patients (10,11) are described elsewhere. Informed consent was obtained from all patients before their participation in this study.

cDNA library screening

We screened 1×10^6 plaques of the full-length kidney cDNA library in λTriplEx (Clontech) by hybridization with probes from exon 2 and the 3′ UTR of the *SOST* gene. Positive clones were converted from λTriplEx to pTriplEx according to the manufacturer's protocol and the inserts were completely sequenced using vector and insert primers.

RACE experiments

5′- and 3′-RACE experiments were performed on kidney cDNA (Human Kidney Marathon-Ready cDNA kit; Clontech) with one adapter primer supplied within the kit and one gene-specific primer. PCR-reactions were carried out using the Advantage 2 PCR kit (Clontech) according to the manufacturer's instructions.

Mutation analysis

Direct sequence analysis was performed on genomic DNA. Each exon was amplified by PCR using primers designed to amplify the two exons including their intron–exon boundaries (exon 1: SOST1F 5′-AgAATTcTcTcTcTccAccc-3′ and SOST1R 5′-gTgcTAcTggAAggTggc-3′ ; exon 2: SOST2F 5′-cgcAgAg-gAcAgAAATgTgg-3′; SOST2R 5′-TcAcgcgcgccTcTcTcc-3′). The sequences of primers used to amplify intronic and flanking fragments are available upon request. PCR products were purified from the agarose gel using the Sephaglas Band-Prep Kit (Pharmacia Biotech). Sequencing reactions, based on the dideoxy sequencing method, were performed using the ABI PRISM BigDye Terminator Cycle Sequencing v2.0 Ready Reaction kit (Perkin Elmer). Fragments were analyzed using an ABI 377 Automated Sequencer.

Controls

We screened a panel of genomic DNA from 100 control individuals by PCR analysis with a modified primer and digestion with *Mbo*I (mutation Trp124X) and PCR analysis and digestion with *Bst*EII (mutation Arg126X), followed by polyacrylamide gel electrophoresis. A total of 100 control individuals were directly sequenced for the presence of the splice site mutation (IVS1+3 A→T).

Expression analysis

Expression levels of *SOST* mRNA in 13 different human tissues (Premium RNA panels I-V Clontech) and primary human osteoblasts extracted from a 41-year-old male Caucasian donor (BioWhittaker, Walkersville, MD) and differentiated for 21 days were determined using quantitative PCR (TaqMan). Reverse transcription of 50 ng of RNA was carried out in duplicate using the TaqMan RT kit with random hexamers as primers (Applied Biosystems) in a GeneAmp PCR System 9600 according to the manufacturer's instructions. TaqMan assays were carried out in an ABI Prism 7700 Sequence Detector System according to the manufacturer's instructions using an *SOST*-specific TaqMan fluoregenic probe that overlaps the exon 1 and 2 junction (*SOST* forward primer 5′-AAcAAcAAgAccAT-gAAccgg-3′; *SOST* reversed primer 5′-cATcggTcAcgTAgcggg-3′; *SOST* fluoregenic TaqMan probe 5′-AAAgAcgTgTccgAgAT-AcAgcTgcc-3′). *SOST* mRNA levels have been normalized to GAPDH expression levels as an endogenous control.

REFERENCES

1. Truswell, A.S. (1958) Osteopetrosis with syndactyly, a morphologic variant of Albers-Schönberg disease. *J. Bone Joint Surg.*, **40**(b), 208–218.
2. Beighton, P. (1988) Sclerosteosis. *J. Med. Genet.*, **25**, 200–203.
3. Beighton, P., Barnard, A., Hamersma, H. and van der Wouden, A., (1984) The syndromic status of sclerosteosis and van Buchem disease. *Clin. Genet.*, **25**, 175–181.
4. Kelly, C.H. and Lawlah, J.W. (1946) Albers-Schönberg disease: a family survey. *Radiology*, **47**, 507–513.
5. Witkop, C.J. (1961) Studies of intrinsic disease in isolates with observations on penetrance and expressivity of certain anatomical traits. In Pruzansky (ed.), *Congenital Anomalies of the Face and Associated Structures*. CC Thomas, Springfield, IL, pp. 291–308.
6. Witkop, C.J. (1965) Genetic diseases of the oral cavity. In Tiecke, R.W. (ed.), *Oral Pathology*. McGraw-Hill, New York, NY, pp. 834–843.
7. Stein, S.A., Witkop, C., Hill, S., Fallon, M.D., Viernstein, L., Gucer, G., McKeever, P., Long, D., Altman, J. and Miller, N.R. (1983) Sclerosteosis: Neurogenetic and pathophysiologic analysis of an American kinship. *Neurology*, **33**, 267–277.
8. Paes-Alves, A.F., Rubin, J.L.C., Cardoso, L. and Rabelo, M.M. (1982) Sclerosteosis: a marker of Dutch ancestry ? *Rev. Bras. Genet.*, **4**, 825–834.
9. Higinbotham, N.L. and Alexander, S.F. (1941) Osteopetrosis: four cases in one family. *Am. J. Surg.*, **53**, 444–454.
10. Tacconi, P., Ferrigno, P., Cocco, L., Cannas, A., Tamburini, G., Bergonzi, P. and Giagheddu, M. (1998) Sclerosteosis: report of a case in a black African man. *Clin. Genet.*, **53**, 497–501.
11. Bueno, M., Olivian, G., Jimenez, A., Garagorri, J.M., Sarria, A., Bueno, A.L. and Ramos, F.J. (1994) Sclerosteosis in a Spanish male: first report in a person of Mediterranean origin. *J. Med. Genet.*, **31**, 976–977.
12. Pietruscka, G. (1958) Weitere Mitteilungen über die Marmorknochenkrankheit (Albers-Schönbergsche Krankheit) nebst Bemerkungen zur Differentialdiagnose. *Klin. Monatsbl. Augenheilkd.*, **132**, 509–525.
13. Sugiura, Y. and Yasuhara, T. (1975) Sclerosteosis. A case report. *J. Bone Joint Surg.*, **57**, 273–277.
14. Van Buchem, F.S.P. (1971) Hyperostosis corticalis generalisata: eight new cases. *Acta Med. Scand.*, **189**, 257–267.
15. Van Buchem, F.S.P., Prick, J.J.G. and Jaspar, H.H.J. (1976) Hyperostosis corticalis generalisata familiaris (van Buchem's disease). In *Excerpta Medica*. American Elsevier Publishing, New York, NY, pp. 1–205.
16. Van Buchem, F.S.P., Hadders, H.N., Hansen, J.F. and Woldring, M.G. (1962) Hyperostosis corticalis generalisata. *Am. J. Med.*, **33**, 387–397.

17. Van Hul, W., Balemans, W., Van Hul, E., Dikkers, F.G., Obee, H., Stokroos, R.J., Hildering, P., Vanhoenacker, F., Van Camp, G. and Willems, P.J. (1998) Van Buchem disease (hyperostosis corticalis generalisata) maps to chrososme 17q12-q21. *Am. J. Hum. Genet.*, **62**, 391–399.

18. Dixon, J.M., Cull, R.E. and Gamble, P. (1982) Two cases of van Buchem's disease. *J. Neurol. Neurosurg. Psychiatry*, **45**, 913–918.

19. Lopez, A.G., Pinero, M.L. and Varo, F.M. (1985) Hiperostosis cortical generalizada (van Buchem). *Rev. Clin. Esp.*, **177**, 293–294.

20. Miguez, A.M., Esteban, B.M., Ramallo, V.G., Quinones, J.M., Hernandez, J.A., Lafuente, J. and Albarran, A.J. (1986) Partial empty sella turcica in van Buchem's disease. *Med. Clin.*, **87**, 719–721.

21. Fryns, J.P. and Van den Berghe, H. (1988) Facial paralysis at the age of 2 months as a first clinical sign of van Buchem disease (endosteal hyperostosis). *Eur. J. Pediatr.*, **147**, 99–100.

22. Cook, J.V., Phelps, P.D. and Chandy, J. (1989) Van Buchem's disease with classical radiological features and appearances on cranial computed tomography. *Br. J. Radiol.*, **62**, 74–77.

23. Bettini, R., Sessa, V., Mingardi, R., Molinari, A., Anzani, P. and Vezzetti, V. (1991) Endosteal hyperostosis with recessive transmission (Van Buchem's disease). A case report. *Recenti Prog. Med.*, **82**, 24–28.

24. Balemans, W., Van Den Ende, J., Paes-Alves, A.F., Dikkers, F.G., Willems, P.J., Vanhoenacker, F., de Almeida-Melo, N., Freire Alves, C., Stratakis, C.A., Hill, S.C. *et al.* (1999) Localization of the gene for sclerosteosis to the van Buchem disease-gene region on chromosome 17q12-q21. *Am. J. Hum. Genet.*, **64**, 1661–1669.

25. Albertsen, H.M., Smith, S.A., Mazoyer, S., Fujimoto, E., Stevens, J., Williams, B., Rodriguez, P., Cropp, C.S., Slijepcevic, P., Carlson, M. *et al.* (1994) A physical map and candidate region in the *BRCA1* region on chromosome 17q12–21. *Nature Genet.*, **7**, 472–479.

26. Neuhausen, S.L., Swensen, J., Miki, Y., Liu, Q., Tavtigian, S., Shattuck-Eidens, D., Kamb, A., Hobbs, M.R., Gingrich, J., Shizuya, H. *et al.* (1994) A P1-based physical map of the region from D17S776 to D17S78 containing the breast cancer susceptibility gene *BRCA1*. *Hum. Mol. Genet.*, **3**, 1919–1926.

27. Froehlich, S., Houlden, H., Rizzu, P., Chakraverty, S., Baker, M., Kwon, J., Nowotny, P., Isaacs, A., Nowotny, V., Wauters, E. *et al.* (1999) Construction of a detailed physical and transcript map of the FTDP-17 candidate region on chromosome 17q21. *Genomics*, **60**, 129–136.

28. Williams, G.W., Woollard, P.M. and Hingamp, P. (1998) NIX: a nucleotide identification system at the HGMP-RC. URL: http://www.hgmp.mrc.ac.uk/NIX/.

29. Shapiro, M.B. and Senapathy, P. (1987) RNA splice junctions of different classes of eukaryotes: sequence statistics and functional implications in gene expression. *Nucleic Acids Res.*, **15**, 7155–7174.

30. Ginsburg, M. (1994) Sequence comparison. In Bishop, M.J. (ed.), *Guide to Human Genome Computing*. Academic Press, New York, NY, pp. 215–248.

31. Emanuelsson, O., Nielsen, H., Brunak, S. and von Heijne, G. (2000) Predicting subcellular localization of proteins based on their N-terminal amino acid sequence. *J. Mol. Biol.*, **300**, 1005–1016.

32. Bateman, A., Birney, E., Durbin, R., Eddy, S.R., Howe, K.L. and Sonnhammer, E.L. (2000) The Pfam protein families database. *Nucleic Acids Res.*, **28**, 263–266.

33. Kleinjan, D.-J. and van Heyningen, V. (1998) Position effect in human genetic disease. *Hum. Mol. Genet.*, **7**, 1611–1618.

34. Kishimoto, T.K., O'Connor, K. and Springer T.A. (1989) Leucocyte adhesion deficiency. *J. Biol. Chem.*, **264**, 3588–3595.

35. Carstens, R.P., Fenton, W.A. and Rosenberg, L.R. (1991) Identification of RNA splicing errors resulting in human ornithine transcarbamylase deficiency. *Am. J. Hum. Genet.*, **48**, 1105–1114.

36. McDonald, N.Q. and Hendrickson, W.A. (1993) A structural superfamily of growth factors containing a cystine knot motif. *Cell*, **73**, 421–424.

37. Bork, P. (1993) The modular architecture of a new family of growth regulators related to connective tissue growth factor. *FEBS Lett.*, **327**, 125–130.

38. Brigstock, D.R. (1999) The connective tissue growth factor/cysteine-rich 61/Nephroblastoma overexpressed (CCN) family. *Endocrinol. Rev.*, **20**, 189–206.

39. Lapthorn, A.J., Harris, D.C., Littlejohn, A., Lustbader, J.W., Canfield, R.E., Machin, K.J., Morgan, F.J. and Isaacs, N.W. (1994) Crystal structure of human chorionic gonadotropin. *Nature*, **369**, 455–461.

40. Hsu, D.R., Economides, A.N., Wang, X., Eimon, P.M. and Harland, R.M. (1998) The *Xenopus* dorsalizing factor gremlin identifies a novel family of secreted proteins that antagonize BMP activities. *Mol. Cell*, **1**, 673–683.